J Shoulder Elbow Surg (2019) 28, 654–664

ELSEVIER

Journal of Shoulder and Elbow Surgery

www.elsevier.com/locate/ymse

The effect of adipose-derived stem cells on enthesis healing after repair of acute and chronic massive rotator cuff tears in rats

Benjamin B. Rothrauff, MD, PhD[a], Catherine A. Smith[b], Gerald A. Ferrer, BS[b], João V. Novaretti, MD[a], Thierry Pauyo, MD[a], Tom Chao, MD[a], David Hirsch, MD[a], Mason F. Beaudry, BS[a], Elmar Herbst, MD[a], Rocky S. Tuan, PhD[a,b], Richard E. Debski, PhD[a,b], Volker Musahl, MD[a,b,*]

[a]*Department of Orthopaedic Surgery, University of Pittsburgh, Pittsburgh, PA, USA*
[b]*Department of Bioengineering, University of Pittsburgh, Pittsburgh, PA, USA*

Background: Chronic massive rotator cuff tears heal poorly and often retear. This study investigated the effect of adipose-derived stem cells (ADSCs) and transforming growth factor-β3 (TGF-β3) delivered in 1 of 2 hydrogels (fibrin or gelatin methacrylate [GelMA]) on enthesis healing after repair of acute or chronic massive rotator cuff tears in rats.

Methods: Adult male Lewis rats underwent bilateral transection of the supraspinatus and infraspinatus tendons with intramuscular injection of botulinum toxin A (n = 48 rats). After 8 weeks, animals received 1 of 8 interventions (n = 12 shoulders/group): (1) no repair, (2) repair only, or repair augmented with (3) fibrin, (4) GelMA, (5) fibrin + ADSCs, (6) GelMA + ADSCs, (7) fibrin + ADSCs + TGF-β3, or (8) GelMA + ADSCs + TGF-β3. An equal number of animals underwent acute tendon transection and immediate application of 1 of 8 interventions. Enthesis healing was evaluated 4 weeks after the repair by microcomputed tomography, histology, and mechanical testing.

Results: Increased bone loss and reduced structural properties were seen in chronic compared with acute tears. Bone mineral density of the proximal humerus was higher in repairs of chronic tears augmented with fibrin + ADSCs and GelMA + ADSCs than in unrepaired chronic tears. Similar improvement was not seen in acute tears. No intervention enhanced histologic appearance or structural properties in acute or chronic tears.

Conclusions: Surgical repair augmented with ADSCs may provide more benefit in chronic tears compared with acute tears, although there was no added benefit to supplementing ADSCs with TGF-β3.

Level of evidence: Basic Science Study; Biomechanics and Histology; In-vivo Animal Model

Keywords: Shoulder; rotator cuff; mesenchymal stem cell; enthesis; chronicity; augmented repair; rat

The University of Pittsburgh Institutional Animal Care and Use Committee approved this study (Protocol #: 1509665)

*Reprint requests: Volker Musahl, MD, UPMC Center for Sports Medicine, 3200 S Water St, Pittsburgh, PA 15203, USA.
E-mail address: musahlv@upmc.edu (V. Musahl).

1058-2746/$ - see front matter
https://doi.org/10.1016/j.jse.2018.08.044

Surgical treatment of chronic massive rotator cuff tears remains a challenge, with repair failure reported in excess of 79% of the most severe cases.[15,28,38] Most rotator cuff tears occur near the tendon-to-bone interface (ie, enthesis), where a gradient of mineralized fibrocartilage normally functions to dissipate the stress concentrations otherwise inherent when compliant tendon attaches to stiff bone.[19,56] The native enthesis structure is not regenerated after surgical repair[43,58]; instead, collagen fibers of the tendon insert directly into bone, predisposing the repair site to failure.[29,35] The repair site of chronic massive cuff tears is further challenged by increased repair tension secondary to muscle degeneration (ie, increased fibrosis and fatty infiltration)[13,23] and reduced bone mineral density (BMD) in the greater tuberosity due to chronic unloading.[5,42]

The delivery of growth factors or cells to the repair site during rotator cuff repair has been investigated in animal models in an effort to restore the structure and function of the native enthesis.[34] Because isoforms of the transforming growth factor-β (TGF-β) family are known mediators of enthesis development and healing,[14,16,18] the effect of delivering exogenous TGF-β to the healing site was previously investigated. In a rodent repair model of an acute supraspinatus tear, controlled release of TGF-β3 from an interpositional scaffold accelerated the healing process, thereby improving mechanical strength at later time points.[39] However, the native fibrocartilage interface was not regenerated, a finding similar to an independent study in which the repair site was augmented with exogenous TGF-β1.[3]

Parallel studies investigated the effect of augmenting rotator cuff repairs with cell-based therapies. The mesenchymal stem cell (MSC) has been most commonly used because it can be isolated from autologous tissues and may contribute to tissue regeneration by differentiating into the appropriate cell phenotype or secreting paracrine factors that enhance healing.[7,54] The effect of MSCs on enthesis regeneration of the rotator cuff has been equivocal,[24,25] with a comprehensive review of preclinical studies suggesting that MSC therapies may be most efficacious when combined with biochemical cues involved in enthesis development, including chondrogenic factors.[45]

To date, most of the studies investigating the effect of growth factors or cells on rotator cuff healing have used a rodent model in which the supraspinatus is acutely transected and immediately repaired, with or without biological augmentation. Although the rodent shoulder most closely matches the anatomy of the human shoulder compared with other quadrupeds,[53] the acute model does not mimic most challenging clinical cases in which tears are chronic.[34] Rodent models of chronic rotator cuff tears, with associated tendon disorganization,[22] muscle degeneration,[33,37,47] bone loss at the humeral head,[17,55] and increased repair tension,[21] were recently developed. As in humans, tear size and chronicity are associated with worsening tissue quality and poorer healing in rats.[30,31,33] Although augmentation of rotator cuff repairs with MSCs and growth factors has shown promise in acute tear models, similar investigations in chronic tear models are largely absent.

The purpose of this study was to evaluate the effect of adipose-derived MSCs (ADSCs), with or without TGF-β3 supplementation, on enthesis healing when augmenting the repair of a chronic massive rotator cuff tear in rats. Augmented repairs of acute tears were performed for comparison. ADSCs and TGF-β3 were localized to the repair site using 1 of 2 hydrogels, fibrin or gelatin methacrylate (GelMA), both of which have been shown to support chondrogenic and tenogenic differentiation of seeded MSCs.[3,4,36] As evaluated by microcomputed tomography (μCT), histology, and mechanical testing, we hypothesized that (1) repair augmentation with combined ADSCs and TGF-β3 would promote superior healing compared with augmentation with ADSCs alone, (2) ADSC-augmented repairs would promote superior healing compared with nonaugmented repairs, and (3) repair augmentation would provide greater benefit in chronic tears compared with acute tears. No differences between repairs augmented with fibrin compared with GelMA were expected.

Materials and methods

Experimental design

Adult, male Lewis rats (n = 110 animals) were used. In a pilot study, 4 rats underwent unilateral shoulder surgery and an equal number underwent bilateral shoulder surgery. Because there were no group differences in postoperative feeding, grooming, or signs of distress, all subsequent animals used in this study underwent bilateral shoulder surgery. We evenly distributed 96 animals to the chronic (n = 48) or acute condition (n = 48), resulting in 96 shoulders per condition.

Animals in the chronic condition initially received bilateral shoulder surgery in which massive rotator cuff tears were created (as described below). After 8 weeks, animals underwent a second operation during which 1 of 8 interventions was performed (n = 12 shoulders/group): (1) no repair, (2) repair only, or repair augmented with (3) fibrin, (4) GelMA, (5) fibrin + ADSCs, (6) GelMA + ADSCs, (7) fibrin + ADSCs + TGF-β3, (8) GelMA + ADSCs + TGF-β3. At 4 weeks postoperatively, animals were humanely killed, and enthesis healing was evaluated by μCT (micro CT), histology, and mechanical testing, as detailed below (Fig. 1). Six rats (12 shoulders) were used as healthy controls and as the source of syngeneic ADSCs.

ADSC isolation and characterization

The rat has 3 principal fat depots: abdominal, testicular, and inguinal (Fig. 2, *A, B*). Inguinal fat was collected from 6 rats and washed in 1× phosphate-buffered saline (Gibco, Gaithersburg, MD, USA). The fat was finely minced with scissors. Approximately 10 cm^3 of fat was placed in a 50-mL conical tube to which was added 40 mL of Hank's Balanced Salt Solution (containing calcium; HyClone, Logan, UT, USA) supplemented with 100 mg of collagenase type I (Worthington Biochemical, Lakewood, NJ, USA) and 100 mg of trypsin IIS (Sigma-Aldrich, St. Louis, MO, USA). Fat was digested for 3 hours at 37°C in an orbital shaker.

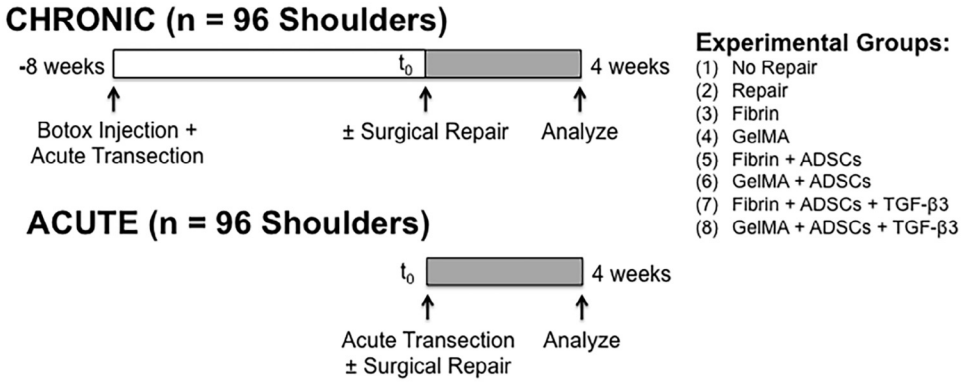

Figure 1 Experimental design. *Botox*, Allergan, Dublin, Ireland; *GelMA*, gelatin methacrylate; *ADSCs*, adipose-derived stem cells; *TGF*, transforming growth factor.

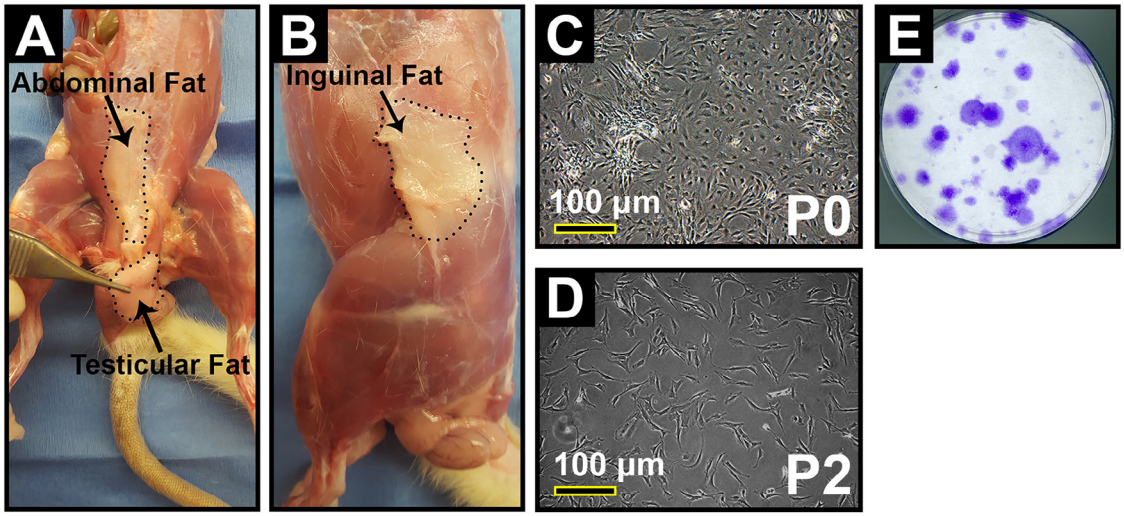

Figure 2 Isolation and characterization of adipose-derived stem cells. Fat depots in rats are found in the (**A**) abdominal, testicular, and (**B**) inguinal region. (**C**) Primary (passage 0 [*P0*]) stromal vascular cells isolated from inguinal fat showed heterogeneous morphologies. (**D**) Spindle-shaped cells at passage 2 (P2) suggested an mesenchymal stem cell phenotype. (**E**) Passage 2 adipose-derived stem cells formed colonies, as shown by crystal violet staining.

The digest was passed through a 250-µm filter then centrifuged at 400*g* for 5 minutes. The resulting pellet was suspended in 25 mL of growth medium consisting of Dulbecco's modified Eagle medium (Thermo Fisher, Pittsburgh, PA, USA), 10% volume/volume (v/v) fetal bovine serum (Thermo Fisher), and 1% v/v antimycotic-antibiotic (Thermo Fisher). The cell suspension was passed through a 100-µm filter and centrifuged at 400*g* for 5 minutes. The pellet was suspended in 3 mL of red blood cell lysis buffer (Sigma-Aldrich) for 10 minutes at room temperature. Then, 47 mL of growth medium was added, the cell suspension centrifuged for 5 minutes at 400*g*, and the resulting pellet was suspended in 25 mL of growth medium supplemented with 1 ng/mL fibroblast growth factor-2 (RayBiotech, Norcross, GA, USA).

Cells were plated in a T150 flask with medium changes every 3 days. At 80% to 90% confluence, cells were passaged. Passage 2 (P2) cells were evaluated for colony-forming capacity and multipotency (ie, adipogenic, chondrogenic, osteogenic differentiation) according to established protocols,[59] with the following modifications: for chondrogenic differentiation, cells were grown in monolayer, as opposed to pellet culture, and the chondrogenic medium was supplemented with human recombinant 10 ng/mL TGF-β3 (PeproTech, Rocky Hill, NJ, USA) rather than TGF-β1.

Hydrogel fabrication

GelMA and a visible-light photoinitiator (lithium phenyl-2,4,6-trimethylbenzoylphosphinate [LAP]) were made as previously described.[36] GelMA was suspended in Hank's Balanced Salt Solution at 10% weight/v. After titrating the pH to 7.4 with 1 N NaOH, 0.15% weight/v LAP and 1% v/v antimycotic-antibiotic were added. The GelMA solution was frozen until use. At the time of the surgery, GelMA was warmed to 37°C. Where indicated, P2 ADSCs were suspended in GelMA at a final concentration of 20×10^6 ADSCs/mL. Similarly, human recombinant TGF-β3 was added to the designated hydrogels at a final concentration of 2.0 µg/mL. At implantation, 50 µL of GelMA construct was pipetted between the tendon and greater tuberosity and exposed to ultraviolet light (390-395 nm, 0.5 W) for 2 minutes to induce in situ gelation.

Plasminogen-depleted fibrinogen (EMD Millipore, Billerica, MA, USA) was suspended in 1× phosphate-buffered saline to a final concentration of 20 mg/mL. As with GelMA constructs, ADSCs or TGF-β3, or both, were suspended in fibrinogen at the time of surgery. To induce in situ gelation, an initiator solution of thrombin (10 U/mL) and $CaCl_2$ (6.9mM) was added. Then, 50 µL of the activated fibrinogen solution was pipetted into the repair site and given 2 minutes to polymerize before sutures were tightened.

Surgical procedure

The surgical procedure was adapted from previous reports.[30,31] To create massive chronic rotator cuff tears, general anesthesia was induced with 4% isoflurane carried by oxygen and maintained with 2% isoflurane. Skin of the shoulders was shaved and sterilized with sequential ethanol and Betadine (Purdue Pharma LP, Stamford, CT, USA) solutions. A 2-cm craniolateral incision was made over the shoulder with a No. 15 blade. The insertions of the supraspinatus and infraspinatus tendons into the greater tuberosity were visualized through a deltoid-splitting approach. Then, 2.5 U (~6 U/kg) Botox (Allergan, Dublin, Ireland) was injected into the muscle bellies. Tendons were sharply transected off the bone by a No. 11 blade, and their retraction under the acromion was visually confirmed. Any remaining insertional fibrocartilage was removed with a burr. Removal of fibrocartilage was confirmed by histology in the pilot study (Supplemental Fig. S1). The deltoid and skin were sequentially closed with 4-0 Vicryl (Ethicon, Somerville, NJ, USA).

During recovery under heat lamps, rats were injected subcutaneously with 0.05 mg/kg buprenorphine, which was subsequently administered every 12 hours for 3 days. Rats were allowed free cage activity and ad libitum diet for 8 weeks, when surgical repair was performed.

Access to the supraspinatus and infraspinatus tendons was gained, as described above. Adhesions between the tendons and surrounding structures were removed. An anteroposterior bone tunnel was drilled through the humeral head just deep to the greater tuberosity using a 22-gauge needle. Both tendons were grasped with a single 5-0 Prolene suture (Ethicon) using a modified Mason-Allen stitch. The suture was then passed through the bone tunnel and partially tightened. If the shoulder was designated for augmented repair, the hydrogel was localized between the tendon and bone, as described above. After gelation, the suture was fully tightened to appose the tendon and greater tuberosity, with or without the interpositional hydrogel. The same surgical approach was used for all animals in the acute condition, excluding the initial surgery to create the iatrogenic massive chronic rotator cuff tear. The postoperative course was the same as previously described. All animals were humanely killed at postoperative week 4 by carbon dioxide asphyxiation.

Shoulders were isolated for further analysis. The supraspinatus and infraspinatus muscles were dissected away from the scapula, and the humeral head was cleaned of all soft tissues, with care taken to preserve the healing tendon-to-bone insertion. Although the supraspinatus and infraspinatus tendons were enveloped in an interdigitated scar mass in all specimens, the native supraspinatus and infraspinatus tendons could be identified and were separated by careful dissection. Bone morphometry of all shoulders (n = 12 shoulders/group) was evaluated by µCT. Of the 12 specimens per condition, 4 were fixed in 10% formalin for histology, and 8 were frozen at –20°C until mechanical testing was performed.

Bone morphometry

Bone morphometry of the proximal humeral epiphysis was evaluated, including the region proximal to growth plate but excluding cortical bone. Bone morphometry specifically at the tendon insertion sites could not be consistently performed with this methodology given the small size of the insertion site, the nominal bone loss that could occur with burring, and the robust scar formation after injury. Measured parameters included BMD, bone volume (BV) percentage (BV/total volume [TV]), and trabeculae number (TbN), thickness (TbTh), and spacing (TbS), and were determined using a µCT 40 system (Scanco USA Inc., Wayne, PA, USA) with 20-µm voxel size at 45 kV/177 µA and 300 ms integration time, as previously described.[30,31]

Histology

Formalin-fixed specimens (n = 4 shoulders/group) were decalcified in formic acid with ethylenediaminetetraacetic acid (Formical2000, Thermo Fisher), serially dehydrated, paraffin embedded, and sectioned in the coronal plane (6 µm thickness) with a Leica RM2255 microtome (Leica Biosystems, Buffalo Grove, IL, USA). Four to 5 sections of each specimen, from anterior to posterior, were rehydrated and stained with hematoxylin and eosin (H&E; Sigma-Aldrich), then imaged using an Olympus SZX16 stereomicroscope (Olympus, Center Valley, PA, USA). Stained sections were evaluated for cellularity, vascularity, foreign bodies, interface disruption, enthesis structure, and collagen (tendon) structure using a semiquantitative scale (see H&E Scoring Parameters in the Supplemental Material) adapted from previously established criteria.[30,31] Samples were scored in a blinded fashion by 2 orthopedic surgeons (T.P., E.H.) familiar with enthesis histology.

Mechanical testing

Fresh frozen specimens (n = 8 shoulders/group) were thawed overnight at room temperature. Specimens were kept moist with physiologic saline solution to prevent dehydration during preparation and testing. Each humerus was potted using epoxy putty and secured in a materials testing machine (Model 5965; Instron, Norwood, MA, USA) equipped with a 50-N load cell. To prevent humeral head avulsion, a cerclage with surgical steel monofilament was performed on the humeral head. To prevent slippage of the supraspinatus tendon during testing, the supraspinatus tendon was superglued in a Kimwipe (Kimberly-Clark Professional, Roswell, GA, USA) and gripped with a custom soft tissue clamp.[30,31,41] The supraspinatus tendon was tested with uniaxial tension, simulating 90° of abduction, ensuring that all fibers were aligned to maximize fiber recruitment.

Before testing, a preload of 0.2 N and preconditioning from 0.2 to 1 N for 10 cycles were applied to the supraspinatus tendon to minimize soft tissue viscoelastic effects. Loading levels used were determined during preliminary tests using intact, healthy tendons.

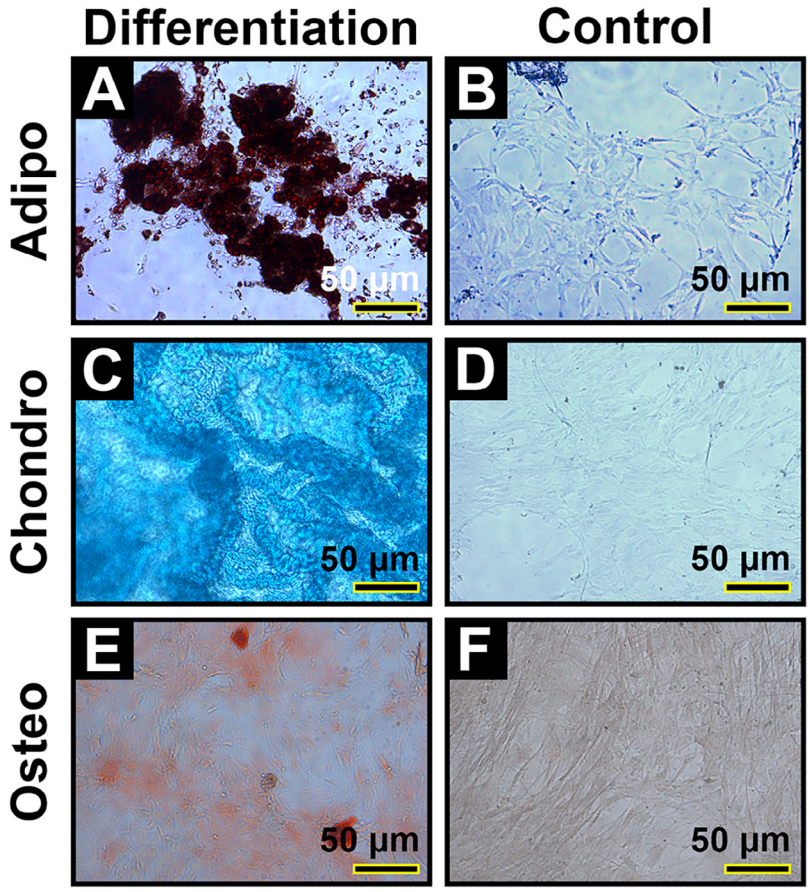

Figure 3 Multipotency of adipose-derived stem cells at passage 2. Adipose-derived stem cells undergo adipogenic (*Adipo*), chondrogenic (*Chondro*) , and osteogenic (*Osteo*) differentiation, as demonstrated by positive staining with (**A**) Oil Red O, (**C**) Alcian Blue, and (**E**) Alizarin Red. (**B, D,** and **F**) Negative staining of cells cultured in control (growth) medium. (For interpretation of the references to colour in this figure legend, the reader is referred to the web version of this article.)

Finally, a load-to-failure test was performed. All testing occurred at an elongation rate of 5 mm/min. Structural properties (ultimate load, ultimate elongation, stiffness, and energy absorption to failure) were determined from the load-elongation curve of the load-to-failure test. Ultimate load and elongation were determined as the maximum load and elongation achieved during the load-to-failure test. Stiffness of the linear region was calculated by iteratively removing the first and last data points of the load-elongation curve until a linear regression fit of $r^2 \geq 0.9$ was achieved. Energy absorption to failure was calculated using trapezoidal numerical integration. Failure modes (enthesis, midsubstance, clamp, or humeral head avulsion) were recorded for each specimen.

Statistical analyses

Statistical analyses were performed using SPSS 22.0 software (IBM, Armonk, NY, USA). A 2-way analysis of variance (2-factor chronicity [acute or chronic] × 8-factor experimental groups) was performed to evaluate for main and interactive effects for parameters of bone morphometry, histology, and structural properties. To corroborate main effects within a chronicity group (acute or chronic), a 1-way analysis of variance with a post hoc Bonferroni correction was performed. A 2-tailed independent *t* test was performed to compare chronic and acute groups. A χ^2 test was performed to evaluate the effect of the hydrogel construct (ie, fibrin vs. GelMA) on failure mode. Significance was set at $P < .05$.

Results

Characterization of ADSCs

The stromal vascular cells isolated from inguinal fat initially demonstrated heterogeneous morphology (P0; Fig. 2, *C*) but possessed spindle-shape morphology consistent with MSCs by P2 (Fig. 2, *D*). P2 ADSCs also demonstrated colony-forming capacity (Fig. 2, *E*) and multipotency by differentiating into adipogenic, chondrogenic, and osteogenic lineages (Fig. 3).

Validation of rodent model of chronic massive rotator cuff tear

Pilot studies confirmed degenerative changes of the tissues comprising the rotator cuff organ, as previously reported. Namely, the supraspinatus and infraspinatus muscles of animals in the chronic condition demonstrated gross atrophy (Fig. 4, *A*), histologic atrophy, and fatty infiltration (Fig. 4, *B*), and

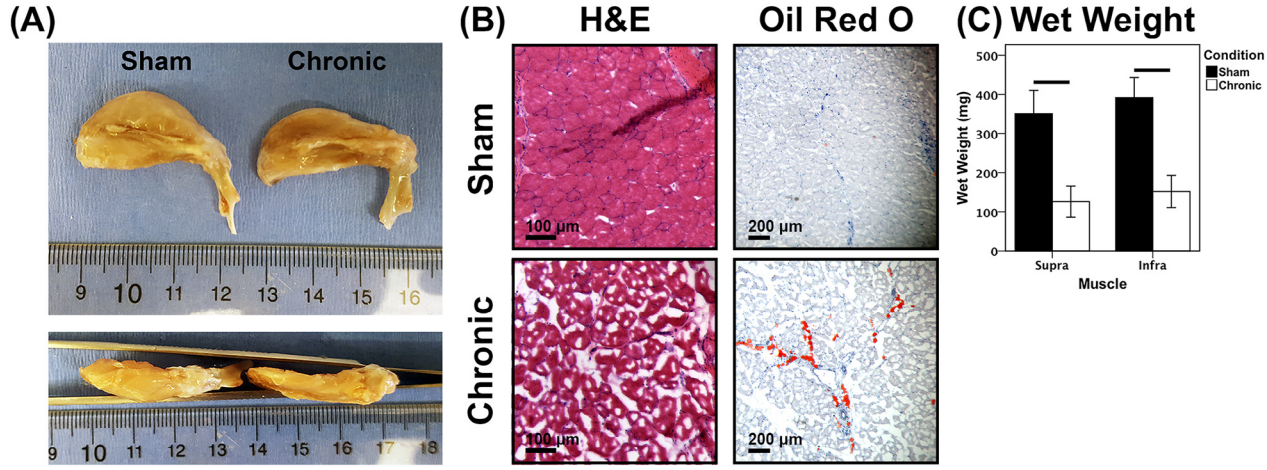

Figure 4 Validation of muscle degeneration in rodent model of chronic massive rotator cuff tear. (**A**) Gross atrophy of supraspinatus and infraspinatus muscles as shown from posterior (top) and superior (bottom) views. (**B**) Hematoxylin and eosin (*H&E*) (left) and Oil Red O (right) staining of muscle in cross-section showing muscle fiber atrophy, disorganization, and fatty deposits (*red* on bottom right). (**C**) Significant reduction in wet weight of supraspinatus and infraspinatus muscles 8 weeks after botulinum toxin A injection and tendon transection compared with sham controls ($P < .05$). Data are presented as the mean and standard deviation (*error bars*). (For interpretation of the references to colour in this figure legend, the reader is referred to the web version of this article.)

Table I Bone morphometry parameters in the control and the experimental groups at 4 weeks after repair with or without augmentation

Condition	Group	BMD[*,†] (μg/mm³)	BV/TV[*,†]	TbN[†,‡] (1/mm)	TbTh (mm)	TbS[†,‡] (mm)
	Control	468.5 ± 14.0	0.428 ± 0.020	3.36 ± 0.4	0.116 ± 0.005	0.286 ± 0.042
Acute	No repair	383.9 ± 30.6	0.324 ± 0.040	3.19 ± 0.20	0.101 ± 0.011	0.352 ± 0.060
	Repair	367.7 ± 35.3	0.304 ± 0.049	3.01 ± 0.28	0.113 ± 0.004	0.347 ± 0.039
	Fibrin	391.7 ± 41.6	0.365 ± 0.040	3.06 ± 0.63	0.108 ± 0.007	0.350 ± 0.092
	GelMA	397.4 ± 28.0	0.333 ± 0.026	3.07 ± 0.56	1.115 ± 0.009	0.343 ± 0.081
	Fibrin + ADSCs	378.7 ± 31.0	0.337 ± 0.027	2.77 ± 0.68	0.120 ± 0.008	0.347 ± 0.130
	GelMA + ADSCs	389.0 ± 20.3	0.335 ± 0.016	3.13 ± 0.51	0.108 ± 0.012	0.336 ± 0.070
	Fibrin + ADSCs + TGF-β	369.0 ± 25.7	0.295 ± 0.022	2.96 ± 0.41	0.115 ± 0.004	0.408 ± 0.102
	GelMA + ADSCs + TGF-β	371.5 ± 55.1	0.321 ± 0.057	2.89 ± 0.77	0.113 ± 0.009	0.388 ± 0.139
Chronic	No repair	284.6 ± 19.3	0.244 ± 0.018	2.11 ± 0.10	0.097 ± 0.011	0.468 ± 0.036
	Repair	295.4 ± 24.1	0.243 ± 0.014	2.39 ± 0.26	0.091 ± 0.012	0.398 ± 0.015
	Fibrin	310.9 ± 10.9	0.233 ± 0.017	2.23 ± 0.58	0.107 ± 0.020	0.476 ± 0.141
	GelMA	320.9 ± 15.4	0.247 ± 0.008	2.28 ± 0.47	0.111 ± 0.011	0.466 ± 0.100
	Fibrin + ADSCs	353.2 ± 18.1[§]	0.256 ± 0.028	2.23 ± 0.31	0.107 ± 0.018	0.453 ± 0.078
	GelMA + ADSCs	354.9 ± 23.5[§]	0.280 ± 0.034	2.28 ± 0.20	0.115 ± 0.018	0.460 ± 0.061
	Fibrin + ADSCs + TGF-β	329.3 ± 27.1	0.257 ± 0.030	2.48 ± 0.24	0.103 ± 0.003	0.416 ± 0.043
	GelMA + ADSCs + TGF-β	339.2 ± 23.2	0.263 ± 0.012	2.23 ± 0.50	0.119 ± 0.008	0.493 ± 0.120

BMD, bone mineral density; *BV/TV*, bone volume/total volume; *TbN*, trabeculae number; *TbTh*, trabeculae thickness; *TbS*, trabeculae spacing; *GelMA*, gelatin methacrylate; *ADSCs*, adipose-derived stem cells; *TGF*, transforming growth factor.
Data are presented as the mean ± standard deviation.
* Groups in both acute and chronic conditions were significantly different from healthy controls ($P < .05$).
† Acute condition was significantly different from the chronic condition ($P < .05$).
‡ Groups in chronic condition were significantly different from healthy controls ($P < .05$).
§ Significantly greater than chronic "no repair" ($P < .01$).

significant reduction in wet weight (Fig. 4, *C*) compared with healthy controls.

Bone morphometry

Compared with healthy controls, the acute and chronic experimental conditions both demonstrated significant reductions in BMD and BV/TV, whereas only the chronic condition demonstrated a significant reduction in TbN and an associated increase in TbS (Table I). For all of these parameters (ie, BMD, BV/TV, TbN, and TbS), the acute condition was significantly different from the chronic condition. There were no differences across any groups for TbTh. When specific interventions within acute and chronic conditions were compared,

Table II Histologic parameters for healthy controls and acute and chronic rotator cuff repairs at 4 weeks after repair with or without augmentation

Condition	Group	Cellularity*,†	Vascularity*	Foreign body*	Interface disruption*	Enthesis structure*	Collagen structure*
	Control	0	0	0	0	0	1
Acute	No repair	2.3 ± 0.8	0.7 ± 0.5	0 ± 0	2.5 ± 0.5	1.7 ± 0.4	2.8 ± 0.3
	Repair	2.7 ± 0.5	1.1 ± 0.4	0 ± 0	2.5 ± 1.1	2.0 ± 0.8	2.8 ± 0.4
	Fibrin	2.3 ± 0.7	0.7 ± 0.4	0.1 ± 0.3	2.7 ± 0.7	1.3 ± 0.6	2.2 ± 0.7
	GelMA	2.3 ± 0.8	0.7 ± 0.4	0 ± 0	2.4 ± 0.7	1.4 ± 0.7	2.4 ± 0.6
	Fibrin + ADSCs	2.8 ± 0.4	1.1 ± 0.4	0 ± 0	1.9 ± 1.1	1.4 ± 0.4	2.7 ± 0.5
	GelMA + ADSCs	2.6 ± 0.5	0.9 ± 0.4	0.1 ± 0.3	2.2 ± 0.8	1.1 ± 0.7	2.2 ± 0.3
	Fibrin + ADSCs + TGF-β	2.7 ± 0.4	0.6 ± 0.4	0.1 ± 0.4	2.6 ± 0.4	1.6 ± 0.6	2.6 ± 0.4
	GelMA + ADSCs + TGF-β	2.6 ± 0.5	0.5 ± 0.4	0.1 ± 0.4	2.7 ± 0.5	1.8 ± 0.5	2.7 ± 0.5
Chronic	No repair	1.4 ± 1.0	0.3 ± 0.4	0 ± 0	2.1 ± 0.7	1.6 ± 0.7	2.2 ± 0.6
	Repair	1.6 ± 1.2	0.8 ± 0.8	0.2 ± 0.4	2.3 ± 1.2	1.3 ± 1.1	2.1 ± 0.8
	Fibrin	2.2 ± 0.9	0.8 ± 0.3	0.9 ± 0.6	2.2 ± 0.9	1.6 ± 0.8	2.6 ± 0.5
	GelMA	2.1 ± 1.0	0.6 ± 0.5	0.1 ± 0.3	1.8 ± 1.1	2.3 ± 0.6	2.4 ± 0.5
	Fibrin + ADSCs	1.3 ± 1.2	0.7 ± 0.6	0 ± 0	2.8 ± 0.3	2.2 ± 0.3	2.2 ± 0.6
	GelMA + ADSCs	1.9 ± 1.3	0.5 ± 0.5	0.2 ± 0.7	2.6 ± 0.7	2.1 ± 0.9	2.6 ± 0.7
	Fibrin + ADSCs + TGF-β	2.2 ± 0.4	0.7 ± 0.4	0.6 ± 0.9	2.4 ± 0.5	2.0 ± 0.0	2.0 ± 0.0
	GelMA + ADSCs + TGF-β	2.4 ± 0.7	0.9 ± 0.3	0.6 ± 1.4	2.4 ± 0.6	1.6 ± 0.5	2.5 ± 0.6

GelMA, gelatin methacrylate; *ADSCs*, adipose-derived stem cells; *TGF*, transforming growth factor.
Data are presented as the mean ± standard deviation.
* Groups in both acute and chronic conditions were significantly different from healthy control ($P < .05$).
† Acute condition was significantly different from chronic condition ($P < .001$).

there was a significantly higher BMD in fibrin + ADSCs (353.2 ± 18.1 μg/mm^3, $P = .011$) and GelMA + ADSCs (354.9 ± 23.5 μg/mm^3, $P = .016$) compared with unrepaired tears (284.6 ± 19.3 μg/mm^3) in the chronic condition.

Histology

The histologic appearance of the enthesis structure was quite variable within groups, limiting interpretation of between-group differences (Supplemental Fig. S2). Compared with the uninjured controls, the acute and chronic conditions were both significantly different in all 6 histologic parameters (Table II). The chronic condition showed significantly less cellularity than the acute condition ($P < .001$). There were no other differences across conditions or among specific interventions within the acute or chronic conditions.

Structural properties

The most common failure mode among all groups was at the enthesis or midsubstance. Repairs augmented with GelMA had a higher failure rate (43.2%) at the enthesis than repairs augmented with fibrin (23.4%, $P = .045$). Midsubstance failure occurred in 44.7% of fibrin-augmented repairs and in 40.9% of GelMA-augmented repairs. The other failures were due to bony avulsions and miscellaneous failure modes. None of the healthy controls failed at the enthesis.

When the chronic condition was compared with the acute condition, chronic tears had significantly lower ultimate load ($P < .001$) and energy absorption to failure ($P = .005$) compared with acute tears. No difference between the experimental groups in the chronic condition was found for ultimate load, ultimate elongation, stiffness, or energy absorption to failure, as shown in Fig. 5. Similar results were found in the acute condition. Ultimate loads ranged from 10 to 13 N and ultimate elongations from 3 to 4 mm. Stiffness did not exceed 6 N/mm for any experimental group, whereas energy absorption to failure was between 10 and 25 N/mm. Healthy controls had a significantly greater ultimate load and stiffness than all experimental groups. The ultimate load and stiffness for controls were, respectively, 248% and 597% greater than the mean values for the chronic condition (Fig. 5). No difference was found between any experimental group and controls for ultimate elongation and energy absorption to failure.

Discussion

This study explored the effects of ADSCs and TGF-β3 delivered in 1 of 2 hydrogels (ie, fibrin or GelMA) on repairs of acute and chronic massive rotator cuff tears in rats. The hypotheses were partially supported, because ADSCs mitigated the loss of BMD in the humeral head in the context of chronic tears, an effect not seen in acute tears. However, ADSCs did not improve the histologic or structural properties of the healing enthesis after repair in acute or chronic tears. Similarly, TGF-β3 supplementation did not further mediate the effect of ADSCs on enthesis healing.

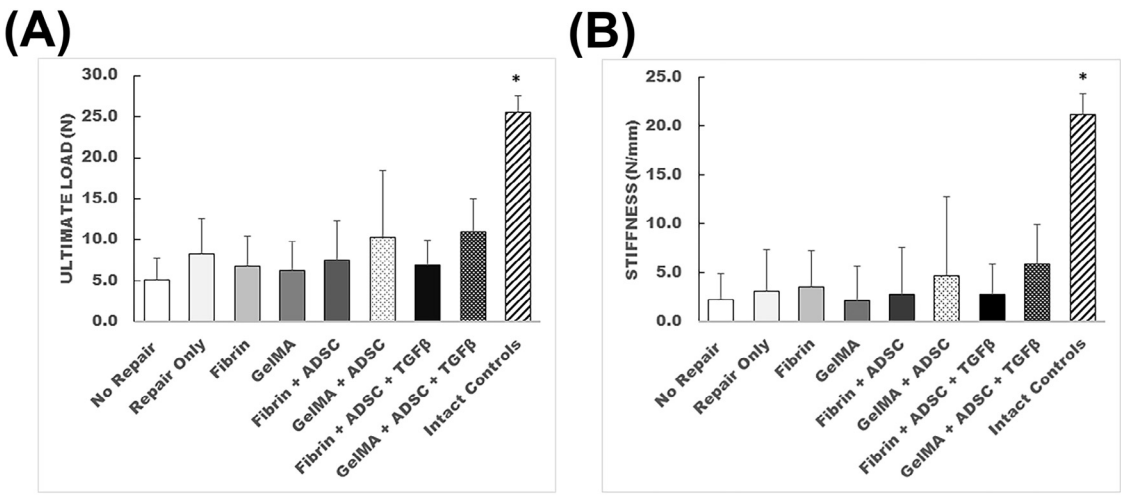

Figure 5 Structural properties of experimental groups in chronic condition. No differences were found between experimental groups with regards to (**A**) ultimate load and (**B**) stiffness. *$P < .05$ indicating all experimental groups were significantly inferior to healthy controls. Data are presented as the mean and standard deviation (*error bars*). *GelMA*, gelatin methacrylate; *ADSCs*, adipose-derived stem cells; *TGF*, transforming growth factor.

The rodent model of a chronic massive tear used in this study developed many of the degenerative changes seen in the corresponding clinical scenario, including decreased BMD in the humeral head and atrophy, fibrosis, and fatty infiltration of the supraspinatus and infraspinatus muscles.[44] These degenerative changes seen in large-to-massive tears are associated with poor healing.[31,38] Accordingly, clinical studies have reported surgical failure rates ranging from 35% to 29% in small-to-medium tears and increasing to 41% to 100% in large-to-massive tears.[11,38,40] Despite the greater clinical need for therapies that improve healing after repair of chronic tears spanning multiple tendons, investigations on the benefits of regenerative strategies (eg, stem cells, scaffolds, growth factors) have largely used animal models in which a single tendon (ie, supraspinatus) is acutely transected and repaired.[8,34] No prior study has compared the effect of MSCs on enthesis healing after repair of acute vs. chronic rotator cuff tears.

At 4 weeks after surgical repair, the BMD of all groups in the chronic condition was significantly reduced compared with the corresponding intervention in the acute condition. However, ADSCs partially mitigated this bone loss in chronic tears. Although investigation of the mechanism by which ADSCs exerted this protective effect was beyond the scope of this study, MSCs are capable of differentiating into osteoblasts or secreting anabolic and anti-inflammatory mediators, or both, that may blunt osteoclast activity at the healing bone-to-tendon interface.[6,26] Under inflammatory conditions, MSCs have been shown to suppress osteoclast formation through the secretion of antiosteoclastogenic factor osteoprotegerin.[51] Furthermore, the MSC secretome contains myriad bioactive factors that modulate chemotaxis, inflammation, cell survival, osteogenic differentiation, and angiogenesis.[2,7,52] ADSC-mediated maintenance of BMD was not associated with improved histologic or structural properties, but these latter properties may have been improved at longer time points. Notably, in a related study in which rats were treated with a pharmacologic agent to activate osteoblastogenesis, significant improvements in BMD and structural properties were not seen until 8 weeks after surgical repair.[50] Additional time points will be explored in future studies.

Although ADSCs mitigated bone loss in chronic tears, regardless of delivery method (ie, fibrin vs. GelMA hydrogel), repairs augmented with GelMA constructs failed at the tendon-to-bone interface more frequently than fibrin constructs. This finding was not expected, because fibrin and GelMA are both cytocompatible hydrogels capable of supporting chondrogenic differentiation of seeded MSCs.[3,4,36] Furthermore, fibrin and gelatin have both been used as interpositional scaffolds to deliver cells or growth factors, or both, to the repair site.[3,24,25] Previously, repairs augmented with fibrin clot were equivalent to nonaugmented repairs of acute rotator cuff tears in a rat model, but a similar comparison had not been performed with GelMA hydrogels.[57] During surgical implementation in this study, we observed that maintenance of the GelMA constructs at the repair site after in situ gelation was more challenging compared with fibrin hydrogels due to poorer tissue adhesivity. The increased frequency of failure at the enthesis in repairs augmented with GelMA constructs may warrant caution if this biomaterial is used as an interpositional scaffold. However, in the context of otherwise equivalent bone morphometry, histology, and structural properties, when comparing repairs augmented with fibrin vs. GelMA constructs, further investigation is needed. Determination of material properties may further clarify a putative advantage of one hydrogel over another.

Contrary to the hypothesis, supplementation of ADSCs with TGF-β3 did not enhance enthesis regeneration. Despite its known role in enthesis development[14] and its conspicuous

absence during intrinsic healing after repair,[18] the augmentation of rotator cuff repairs with exogenous TGF-β3 has yielded equivocal results, including reports of benefit[39] and no effect.[32] The mechanisms underlying the ineffectiveness of TGF-β3 supplementation in this study are unknown but may be attributable to insufficient dosing, poor interspecies homology (ie, the use of human recombinant TGF-β3), the innate, robust scar response in rodents, or the failure to recapitulate its developmental role, among others. TGF-β3 is expressed in a unique temporospatial pattern among other molecular mediators during development. The absence of these other mediators inherent in development, deviating in space or time, or the presence of inflammatory mediators,[1] may negate the bioactivity of exogenous TGF-β3 applied at the time of surgical repair.

Mechanical loading of the developing or healing enthesis, as mediated by muscular contractions, is also known to play a central role in enthesis maturation and healing.[9,48,49] In larger animal models of chronic rotator cuff tears, including rabbit[20] and sheep,[12] the detached tendon is often wrapped in a bioinert sheath (eg, Gore-Tex; W. L. Gore & Associates, Flagstaff, AZ, USA) to prevent scarring of the tendon to adjacent tissues. This mimics the minimal healing response seen in human shoulders, with resulting musculotendinous unloading thought to be the principal cause of muscle degeneration. Despite the robust fibrovascular scar formation that occurs in the rat shoulder after tendon detachment, few rodent models of chronic rotator cuff tears have used a bioinert sheath. Surgical release of the rat tendon(s) alone has been shown sufficient to induce reductions in humeral BMD,[10,17] loss of tendon organization,[55] and increased fibrosis and fatty infiltration of muscles.[33,37] However, these degenerative changes are further exacerbated by denervation (by nerve transection[33,37] or botulinum toxin injection[46,47]) or the prevention of scar formation,[27] suggesting that the passive muscle tension subsequent to scar formation mitigates the severity of musculotendinous degeneration and represents a limitation of the rodent model. For that reason, tendon transection and chemical denervation were concurrently used in the rodent model used in this study, which successfully induced the histopathologic changes seen in human patients. However, suprascapular neuropathy is infrequently found in clinical cases of chronic massive rotator cuff tears, highlighting an additional limitation of this model.

In addition to the inherent limitations of this and other animal models, this study had several limitations. Although enthesis structure was evaluated by adopting an established semiquantitative scoring system, additional measures to evaluate collagen organization (eg, polarized light microscopy) and biochemical composition (eg, immunohistochemistry) at the healing enthesis were not performed. Similarly, only structural properties were obtained. Secondly, ADSCs were not labeled, which would have permitted the analysis of cell retention at the healing site over time. Lastly, only a single time point was used to analyze healing.

Conclusions

This study explored the effects of ADSCs and TGF-β3 delivered in 1 of 2 hydrogels (ie, fibrin or GelMA) on repairs of acute and chronic massive rotator cuff tears in rats. Regardless of delivery method, ADSCs mitigated bone loss at the proximal humeral epiphysis in chronic as opposed to acute tears in a rodent model; this suggests that tear chronicity may mediate the efficacy of cell-based therapies. Repairs augmented with GelMA constructs also failed more frequently at the tendon-to-bone interface, warranting consideration when using this material as an interpositional scaffold to improve enthesis healing. No experimental intervention significantly improved the histologic appearance or structural properties in the acute or chronic conditions. Further investigation is warranted to better understand how stem cell therapies, with or without growth factor supplementation, might be optimized to enhance healing of chronic rotator cuff tears.

Acknowledgments

We thank Dr Jian Tan for her assistance with the characterization of ADSCs.

Disclaimer

This study was funded by the University of Pittsburgh Physicians (UPP)/University of Pittsburgh Medical Center (UPMC) Academic Foundation.

The authors, their immediate families, and any research foundation with which they are affiliated have not received any financial payments or other benefits from any commercial entity related to the subject of this article.

Supplementary data

Supplementary data to this article can be found online at https://doi.org/10.1016/j.jse.2018.08.044

References

1. Abraham AC, Shah SA, Thomopoulos S. Targeting inflammation in rotator cuff tendon degeneration and repair. Tech Shoulder Elb Surg 2017;18:84-90. http://dx.doi.org/10.1097/bte.0000000000000124
2. Ando Y, Matsubara K, Ishikawa J, Fujio M, Shohara R, Hibi H, et al. Stem cell-conditioned medium accelerates distraction osteogenesis through multiple regenerative mechanisms. Bone 2014;61:82-90. http://dx.doi.org/10.1016/j.bone.2013.12.029
3. Arimura H, Shukunami C, Tokunaga T, Karasugi T, Okamoto N, Taniwaki T, et al. TGF-beta 1 improves biomechanical strength by extracellular matrix accumulation without increasing the number of tenogenic lineage cells in a rat rotator cuff repair model. Am J Sports Med 2017;45:2394-404. http://dx.doi.org/10.1177/0363546517707940

4. Breidenbach AP, Dyment NA, Lu YH, Rao M, Shearn JT, Rowe DW, et al. Fibrin gels exhibit improved biological, structural, and mechanical properties compared with collagen gels in cell-based tendon tissue-engineered constructs. Tissue Eng Part A 2015;21:438-50. http://dx.doi.org/10.1089/ten.tea.2013.0768
5. Cadet ER, Hsu JW, Levine WN, Bigliani LU, Ahmad CS. The relationship between greater tuberosity osteopenia and the chronicity of rotator cuff tears. J Shoulder Elbow Surg 2008;17:73-7. http://dx.doi.org/10.1016/j.jse.2007.04.017
6. Caplan AI. Adult mesenchymal stem cells for tissue engineering versus regenerative medicine. J Cell Physiol 2007;213:341-7. http://dx.doi.org/10.1002/jcp.21200
7. Caplan AI, Correa D. The MSC: an injury drugstore. Cell Stem Cell 2011;9:11-5. http://dx.doi.org/10.1016/j.stem.2011.06.008
8. Carballo CB, Lebaschi A, Rodeo SA. Cell-based approaches for augmentation of tendon repair. Tech Shoulder Elb Surg 2017;18:E6-14. http://dx.doi.org/10.1097/bte.0000000000000132
9. Carbone A, Carballo C, Ma R, Wang HS, Deng XH, Dahia C, et al. Indian hedgehog signaling and the role of graft tension in tendon-to-bone healing: evaluation in a rat ACL reconstruction model. J Orthop Res 2016;34:641-9. http://dx.doi.org/10.1002/jor.23066
10. Cavinatto L, Malavolta EA, Pereira CA, Miranda-Rodrigues M, Silva LC, Gouveia CH, et al. Early versus late repair of rotator cuff tears in rats. J Shoulder Elbow Surg 2018;27:606-13. http://dx.doi.org/10.1016/j.jse.2017.10.025
11. Charousset C, Bellaïche L, Kalra K, Petrover D. Arthroscopic repair of full-thickness rotator cuff tears: is there tendon healing in patients aged 65 years or older? Arthroscopy 2010;26:302-9. http://dx.doi.org/10.1016/j.arthro.2009.08.027
12. Coleman SH, Fealy S, Ehteshami JR, MacGillivray JD, Altchek DW, Warren RF, et al. Chronic rotator cuff injury and repair model in sheep. J Bone Joint Surg Am 2003;85A:2391-402.
13. Davidson PA, Rivenburgh DW. Rotator cuff repair tension as a determinant of functional outcome. J Shoulder Elbow Surg 2000;9:502-6.
14. Galatz L, Rothermich S, VanderPloeg K, Petersen B, Sandell L, Thomopoulos S. Development of the supraspinatus tendon-to-bone insertion: localized expression of extracellular matrix and growth factor genes. J Orthop Res 2007;25:1621-8. http://dx.doi.org/10.1002/jor.20441
15. Galatz LM, Ball CM, Teefey SA, Middleton WD, Yamaguchi K. The outcome and repair integrity of completely arthroscopically repaired large and massive rotator cuff tears. J Bone Joint Surg Am 2004;86A:219-24. http://dx.doi.org/10.2106/00004623-200402000-00002
16. Galatz LM, Gerstenfeld L, Heber-Katz E, Rodeo SA. Tendon regeneration and scar formation: the concept of scarless healing. J Orthop Res 2015;33:823-31. http://dx.doi.org/10.1002/jor.22853
17. Galatz LM, Rothermich SY, Zaegel M, Silva MJ, Havlioglu N, Thomopoulos S. Delayed repair of tendon to bone injuries leads to decreased biomechanical properties and bone loss. J Orthop Res 2005;23:1441-7. http://dx.doi.org/10.1016/j.orthres.2005.05.005
18. Galatz LM, Sandell LJ, Rothermich SY, Das R, Mastny A, Havlioglu N, et al. Characteristics of the rat supraspinatus tendon during tendon-to-bone healing after acute injury. J Orthop Res 2006;24:541-50. http://dx.doi.org/10.1002/jor.20067
19. Genin GM, Kent A, Birman V, Wopenka B, Pasteris JD, Marquez PJ, et al. Functional grading of mineral and collagen in the attachment of tendon to bone. Biophys J 2009;97:976-85. http://dx.doi.org/10.1016/j.bpj.2009.05.043
20. Gilotra M, Thao N, Christian M, Davis D, Henn RF 3rd, Hasan SA. Botulinum toxin is detrimental to repair of a chronic rotator cuff tear in a rabbit model. J Orthop Res 2015;33:1152-7. http://dx.doi.org/10.1002/jor.22836
21. Gimbel JA, Van Kleunen JP, Lake SP, Williams GR, Soslowsky LJ. The role of repair tension on tendon to bone healing in an animal model of chronic rotator cuff tears. J Biomech 2007;40:561-8. http://dx.doi.org/10.1016/j.jbiomech.2006.02.010
22. Gimbel JA, Van Kleunen JP, Mehta S, Perry SM, Williams GR, Soslowsky LJ. Supraspinatus tendon organizational and mechanical properties in a chronic rotator cuff tear animal model. J Biomech 2004;37:739-49. http://dx.doi.org/10.1016/j.jbiomech.2003.09.019
23. Godeneche A, Elia F, Kempf JF, Nich C, Berhouet J, Saffarini M, et al. Fatty infiltration of stage 1 or higher significantly compromises long-term healing of supraspinatus repairs. J Shoulder Elbow Surg 2017;26:1818-25. http://dx.doi.org/10.1016/j.jse.2017.03.024
24. Gulotta LV, Kovacevic D, Ehteshami JR, Dagher E, Packer JD, Rodeo SA. Application of bone marrow-derived mesenchymal stem cells in a rotator cuff repair model. Am J Sports Med 2009;37:2126-33. http://dx.doi.org/10.1177/0363546509339582
25. Gulotta LV, Kovacevic D, Packer JD, Deng XH, Rodeo SA. Bone marrow-derived mesenchymal stem cells transduced with scleraxis improve rotator cuff healing in a rat model. Am J Sports Med 2011;39:1282-9. http://dx.doi.org/10.1177/0363546510395485
26. Harris MT, Butler DL, Boivin GP, Florer JB, Schantz EJ, Wenstrup RJ. Mesenchymal stem cells used for rabbit tendon repair can form ectopic bone and express alkaline phosphatase activity in constructs. J Orthop Res 2004;22:998-1003. http://dx.doi.org/10.1016/j.orthres.2004.02.012
27. Hashimoto E, Ochiai N, Kenmoku T, Sasaki Y, Yamaguchi T, Kijima T, et al. Macroscopic and histologic evaluation of a rat model of chronic rotator cuff tear. J Shoulder Elbow Surg 2016;25:2025-33. http://dx.doi.org/10.1016/j.jse.2016.04.024
28. Henry P, Wasserstein D, Park S, Dwyer T, Chahal J, Slobogean G, et al. Arthroscopic repair for chronic massive rotator cuff tears: a systematic review. Arthroscopy 2015;31:2472-80. http://dx.doi.org/10.1016/j.arthro.2015.06.038
29. Jensen PT, Lambertsen KL, Frich LH. Assembly, maturation, and degradation of the supraspinatus enthesis. J Shoulder Elbow Surg 2018;27:739-50. http://dx.doi.org/10.1016/j.jse.2017.10.030
30. Killian ML, Cavinatto L, Shah SA, Sato EJ, Ward SR, Havlioglu N, et al. The effects of chronic unloading and gap formation on tendon-to-bone healing in a rat model of massive rotator cuff tears. J Orthop Res 2014;32:439-47. http://dx.doi.org/10.1002/jor.22519
31. Killian ML, Cavinatto LM, Ward SR, Havlioglu N, Thomopoulos S, Galatz LM. Chronic degeneration leads to poor healing of repaired massive rotator cuff tears in rats. Am J Sports Med 2015;43:2401-10. http://dx.doi.org/10.1177/0363546515596408
32. Kim HM, Galatz LM, Das R, Havlioglu N, Rothermich SY, Thomopoulos S. The role of transforming growth factor beta isoforms in tendon-to-bone healing. Connect Tissue Res 2011;52:87-98. http://dx.doi.org/10.3109/03008207.2010.483026
33. Kim HM, Galatz LM, Lim C, Havlioglu N, Thomopoulos S. The effect of tear size and nerve injury on rotator cuff muscle fatty degeneration in a rodent animal model. J Shoulder Elbow Surg 2012;21:847-58. http://dx.doi.org/10.1016/j.jse.2011.05.004
34. Lebaschi A, Deng XH, Zong JC, Cong GT, Carballo CB, Album ZM, et al. Animal models for rotator cuff repair. Ann N Y Acad Sci 2016;1383:43-57. http://dx.doi.org/10.1111/nyas.13203
35. Leung KS, Chong WS, Chow DH, Zhang P, Cheung WH, Wong MW, et al. A comparative study on the biomechanical and histological properties of bone-to-bone, bone-to-tendon, and tendon-to-tendon healing: an achilles tendon-calcaneus model in goats. Am J Sports Med 2015;43:1413-21. http://dx.doi.org/10.1177/0363546515576904
36. Lin H, Cheng AW, Alexander PG, Beck AM, Tuan RS. Cartilage tissue engineering application of injectable gelatin hydrogel with in situ visible-light-activated gelation capability in both air and aqueous solution. Tissue Eng Part A 2014;20:2402-11. http://dx.doi.org/10.1089/ten.TEA.2013.0642
37. Liu XH, Manzano G, Kim HT, Feeley BT. A rat model of massive rotator cuff tears. J Orthop Res 2011;29:588-95. http://dx.doi.org/10.1002/jor.21266
38. Mall NA, Tanaka MJ, Choi LS, Paletta GA Jr. Factors affecting rotator cuff healing. J Bone Joint Surg Am 2014;96A:778-88. http://dx.doi.org/10.2106/jbjs.m.00583
39. Manning CN, Kim HM, Sakiyama-Elbert S, Galatz LM, Havlioglu N, Thomopoulos S. Sustained delivery of transforming growth factor beta

three enhances tendon-to-bone healing in a rat model. J Orthop Res 2011;29:1099-105. http://dx.doi.org/10.1002/jor.21301
40. Mihata T, Watanabe C, Fukunishi K, Ohue M, Tsujimura T, Fujiwara K, et al. Functional and structural outcomes of single-row versus double-row versus combined double-row and suture-bridge repair for rotator cuff tears. Am J Sports Med 2011;39:2091-8. http://dx.doi.org/10.1177/0363546511415660
41. Newton MD, Davidson AA, Pomajzl R, Seta J, Kurdziel MD, Maerz T. The influence of testing angle on the biomechanical properties of the rat supraspinatus tendon. J Biomech 2016;49:4159-63. http://dx.doi.org/10.1016/j.jbiomech.2016.11.003
42. Oh JH, Song BW, Lee YS. Measurement of volumetric bone mineral density in proximal humerus using quantitative computed tomography in patients with unilateral rotator cuff tear. J Shoulder Elbow Surg 2014;23:993-1002. http://dx.doi.org/10.1016/j.jse.2013.09.024
43. Rodeo SA, Arnoczky SP, Torzilli PA, Hidaka C, Warren RF. Tendon healing in a bone tunnel—a biomechanical and histological study in the dog. J Bone Joint Surg Am 1993;75A:1795-803.
44. Rothrauff BB, Pauyo T, Debski RE, Rodosky MW, Tuan RS, Musahl V. The rotator cuff organ: integrating developmental biology, tissue engineering, and surgical considerations to treat chronic massive rotator cuff tears. Tissue Eng Part B Rev 2017;23:318-35. http://dx.doi.org/10.1089/ten.teb.2016.0446
45. Rothrauff BB, Tuan RS. Cellular therapy in bone-tendon interface regeneration. Organogenesis 2014;10:13-28. http://dx.doi.org/10.4161/org.27404
46. Sato EJ, Killian ML, Choi AJ, Lin E, Choo AD, Rodriguez-Soto AE, et al. Architectural and biochemical adaptations in skeletal muscle and bone following rotator cuff injury in a rat model. J Bone Joint Surg Am 2015;97A:565-73. http://dx.doi.org/10.2106/jbjs.m.01503
47. Sato EJ, Killian ML, Choi AJ, Lin E, Esparza MC, Galatz LM, et al. Skeletal muscle fibrosis and stiffness increase after rotator cuff tendon injury and neuromuscular compromise in a rat model. J Orthop Res 2014;32:1111-6. http://dx.doi.org/10.1002/jor.22646
48. Schwartz AG, Lipner JH, Pasteris JD, Genin GM, Thomopoulos S. Muscle loading is necessary for the formation of a functional tendon enthesis. Bone 2013;55:44-51. http://dx.doi.org/10.1016/j.bone.2013.03.010
49. Schwartz AG, Long FX, Thomopoulos S. Enthesis fibrocartilage cells originate from a population of Hedgehog-responsive cells modulated by the loading environment. Development 2015;142:196-206. http://dx.doi.org/10.1242/dev.112714
50. Shah SA, Kormpakis I, Havlioglu N, Ominsky MS, Galatz LM, Thomopoulos S. Sclerostin antibody treatment enhances rotator cuff tendon-to-bone healing in an animal model. J Bone Joint Surg Am 2017;99:855-64. http://dx.doi.org/10.2106/jbjs.16.01019
51. Sharaf-Eldin WE, Abu-Shahba N, Mahmoud M, El-Badri N. The modulatory effects of mesenchymal stem cells on osteoclastogenesis. Stem Cells Int 2016;2016:1908365. http://dx.doi.org/10.1155/2016/1908365
52. Shen MD, Wu RH, Jin RL, Pan J, Guo F, Li ZY, et al. Injection of synthetic mesenchymal stem cell mitigates osteoporosis in rats after ovariectomy. J Cell Mol Med 2018;22:3751-7. http://dx.doi.org/10.1111/jcmm.13618
53. Soslowsky LJ, Carpenter JE, DeBano CM, Banerji I, Maolli MR. Development and use of an animal model for investigations on rotator cuff disease. J Shoulder Elbow Surg 1996;5:383-92.
54. Steinert AF, Rackwitz L, Gilbert F, Nöth U, Tuan RS. Concise review: the clinical application of mesenchymal stem cells for musculoskeletal regeneration: current status and perspectives. Stem Cells Transl Med 2012;1:237-47. http://dx.doi.org/10.5966/sctm.2011-0036
55. Thangarajah T, Henshaw F, Sanghani-Kerai A, Lambert SM, Pendegrass CJ, Blunn GW. Supraspinatus detachment causes musculotendinous degeneration and a reduction in bone mineral density at the enthesis in a rat model of chronic rotator cuff degeneration. Shoulder Elbow 2017;9:178-87. http://dx.doi.org/10.1177/1758573217696450
56. Thomopoulos S, Marquez JP, Weinberger B, Birman V, Genin GM. Collagen fiber orientation at the tendon to bone insertion and its influence on stress concentrations. J Biomech 2006;39:1842-51. http://dx.doi.org/10.1016/j.jbiomech.2005.05.021
57. Thomopoulos S, Soslowsky LJ, Flanagan CL, Tun S, Keefer CC, Mastaw J, et al. The effect of fibrin clot on healing rat supraspinatus tendon defects. J Shoulder Elbow Surg 2002;11:239-47. http://dx.doi.org/10.1067/mse.2002.122228
58. Thomopoulos S, Williams GR, Soslowsky LJ. Tendon to bone healing: differences in biomechanical, structural, and compositional properties due to a range of activity levels. J Biomech Eng 2003;125:106-13. http://dx.doi.org/10.1115/1.1536660
59. Tuli R, Tuli S, Nandi S, Wang ML, Alexander PG, Haleem-Smith H, et al. Characterization of multipotential mesenchymal progenitor cells derived from human trabecular bone. Stem Cells 2003;21:681-93. http://dx.doi.org/10.1634/stemcells.21-6-681